Nuclear Instruments and Methods in Physics Research A297 (1990) 343–353
North-Holland

The computation of aberrations of fringing fields of magnetic multipoles and sector magnets using differential algebra

B. Hartmann, M. Berz and H. Wollnik

II. Physikalisches Institut der Justus-Liebig-Universität, W-6300 Giessen, Germany

Received 19 January 1990 and in revised form 30 May 1990

Differential algebraic (DA) methods are used for the computation of transfer matrices of arbitrary order of the fringing fields of magnetic particle-optical elements. The accuracy of the method is only limited by the numerical integrator for the equations of motion. Comparisons are made to the method of fringing-field integrals, the results of which are known to third order, and it is shown that the results of both methods agree well.

1. Introduction

In the simulation of particle-optical elements one is often not interested in the trajectories of individual particles, but rather in some global properties of an optical system. Such properties advantageously are described by a nonlinear map relating final phase-space coordinates r_f to initial ones r_i of individual charged particles:

$$r_f = \mathcal{M}(r_i). \tag{1}$$

This transfer map is usually represented by a power series to a prespecified order, the so-called transfer matrix of that order [1,2].

In case of the main fields of particle-optical elements, direct analytical formulas for the expansion coefficients have been found to second [3–6] and to third order [7–11]. Recently, this procedure has been extended to fifth order using a custom-made formula manipulator [12,13].

However, in the case of fringing fields, analytical solutions for the expansion coefficients can be found only for special cases [14]. Thus fringing fields have usually been neglected, treated only as a steep rise function or been only roughly approximated. The best solution so far was to treat them in a perturbative method based on the technique of fringing-field integrals [15–18] which is also used in some ion-optical programs [19–23]. This technique is quite accurate. However, because it simply truncates the action of the fringing field at terms of third order in Δ, the length of the fringing field, it only approximates the symplectic symmetry [24,25] which the system has because it is governed by a Hamiltonian to that accuracy.

Here we present a new method to obtain expansion coefficients for fringing fields to arbitrary order. To do this, we note that the matrix elements or expansion coefficients of the transfer map are simply partial derivatives of the map (see for instance ref. [26]). Using the technique of differential algebra [27–29], which allows an accurate arithmetical computation of derivatives, one thus can compute all elements of a transfer matrix in a consistent way. In this context it is important to note that the corresponding programming effort is independent of the order to which the matrix elements are calculated.

2. Differential algebra

Differential algebraic (DA) methods are related to nonstandard [30] analysis. A detailed description of the method is given in refs. [29,31,32]. Here we illustrate only the simplest DA which will eventually allow the computation of only first-order derivatives and functions of only one variable.

Consider the vector space R^2 of ordered pairs (u_0, u_1), $u_0, u_1 \in R$ in which an addition and a scalar multiplication are defined in the usual way:

$$(u_0, u_1) + (v_0, v_1) = (u_0 + v_0, u_1 + v_1),$$

$$t \cdot (u_0, u_1) = (t \cdot u_0, t \cdot u_1)$$

for $u_0, u_1, v_0, v_1, t \in R$ as well as a multiplication between vectors:

$$(u_0, u_1) \cdot (v_0, v_1) = (u_0 \cdot v_0, u_0 \cdot v_1 + u_1 \cdot v_0)$$

so that the set of ordered pairs becomes an algebra.

When evaluating a function in DA instead of using real numbers, one automatically obtains not only the value of the function, but also its derivatives to a

prespecified order. Note also that all arithmetic functions based on power series can be generalized to DA using coordinatewise convergence. The accuracy of determining derivatives in this manner is always close to machine precision, contrary to numerical techniques [33] in which derivatives are obtained as differences of close numbers. The DA method can be generalized to allow computation of derivatives of higher orders and more than one variable, which is necessary to compute high-order transfer matrices.

3. Transfer matrices obtained by using differential algebra

Without having analytical formulas that relate the final phase-space coordinates r_f to the initial ones r_i, it still is possible to computationally relate the r_f to the r_i by numerically integrating the equations of motion. A particle trajectory can thus be determined from a differential equation of the form

$$\frac{\mathrm{d}}{\mathrm{d}s}\boldsymbol{r} = \boldsymbol{F}(\boldsymbol{r}, s), \tag{2}$$

where s is the independent variable, and where $\boldsymbol{F}$ describes all the forces due to the external and internal electromagnetic fields. To be more specific, we could use the frequently used particle optical coordinates [26]

$$\begin{aligned}
r_1 &= x,\\
r_2 &= a = p_x/p_0,\\
r_3 &= y,\\
r_4 &= b = p_y/p_0,\\
r_5 &= l = v_0(t - t_0),\\
r_6 &= \delta_K = (K/q - K_0/q_0)/(K_0/q_0),\\
r_7 &= \delta_m = (m/q - m_0/q_0)/(m_0/q_0),
\end{aligned} \tag{3}$$

where x and y are the horizontal and vertical distances to the optic axis, respectively, while p_0, v_0, q_0, K_0, m_0 and t_0 denote momentum, velocity, charge, kinetic energy, mass and flight time of the reference particle, whereas p, v, q, K, m and t stand for the same quantities of the particle under consideration. In these coordinates the equations of motion in electromagnetic fields $\boldsymbol{E}$ and $\boldsymbol{B}$ of the described particle take the form [12]:

$$\begin{aligned}
x' &= a(1 + hx)(p_0/\bar{p}),\\
y' &= b(1 + hx)(p_0/\bar{p}),\\
l' &= (1 + hx)(v_0/v)(p/\bar{p}),\\
a' &= \frac{q/q_0}{\chi_B}\left(B_z b\frac{T_0}{T} - B_y\frac{\bar{v}}{v_0}\right)\cdot l' + h\frac{\bar{p}}{p_0},\\
b' &= \frac{q/q_0}{\chi_B}\left(-B_z a\frac{T_0}{T} + B_x\frac{\bar{v}}{v_0}\right)\cdot l'.
\end{aligned} \tag{4}$$

Here $h = 1/\rho$ is the momentary radius of curvature of the optic axis and $\chi_B = p_0/q_0$ is the magnetic rigidity of a reference particle. Furthermore we used the abbreviations

$$\bar{p} = p\sqrt{1 - (p_0/p)^2(a^2 + b^2)}$$

and

$$\bar{v} = v\sqrt{1 - (v_0/v)^2(T_0/T)^2(a^2 + b^2)}$$

as well as

$$\begin{aligned}
\frac{T}{T_0} &= \frac{q}{q_0}\left(1 + \frac{2\eta\delta_K + \delta_m}{1 + 2\eta}\right),\\
\frac{p}{p_0} &= \frac{q}{q_0}\sqrt{(1 + \delta_k)\left(1 + \frac{\eta\delta_K + \delta_m}{1 + \eta}\right)},\\
\frac{v}{v_0} &= \sqrt{(1 + \delta_K)\left(1 + \frac{\eta\delta_K + \delta_m}{1 + \eta}\right)}\Bigg/\left(1 + \frac{2\eta\delta_K + \delta_m}{1 + 2\eta}\right),
\end{aligned} \tag{5}$$

where the factor $\eta = K_0/2m_0c^2$ is used for relativistic corrections with c denoting the speed of light.

Numerical integrators now use the right hand side of eq. (2) to obtain an approximate estimate for the new value of $\boldsymbol{r}$ at the new value of the independent variable $s + \Delta s$. For instance, in the case of the well-known fourth-order Runge–Kutta integrator, the procedure is as follows. After computing quantities k_1, k_2, k_3, k_4 recursively as

$$\begin{aligned}
\boldsymbol{k}_1 &= \boldsymbol{F}(\boldsymbol{r}, s)\cdot\Delta s,\\
\boldsymbol{k}_2 &= \boldsymbol{F}\left(\boldsymbol{r} + \tfrac{1}{2}\boldsymbol{k}_1, s + \tfrac{1}{2}\Delta\right)\cdot\Delta s,\\
\boldsymbol{k}_3 &= \boldsymbol{F}\left(\boldsymbol{r} + \tfrac{1}{2}\boldsymbol{k}_2, s + \tfrac{1}{2}\Delta s\right)\cdot\Delta s,\\
\boldsymbol{k}_4 &= \boldsymbol{F}(\boldsymbol{r} + \boldsymbol{k}_3, s + \Delta s)\cdot\Delta s,
\end{aligned} \tag{6}$$

one obtains from these $\boldsymbol{k}_i$ recursively as an approximate (and for reasonably small Δs usually very good) estimate for the value of $\boldsymbol{r}$ at $s + \Delta s$:

$$\boldsymbol{r}(s + \Delta s) = \boldsymbol{r}(s) + \tfrac{1}{6}\cdot(\boldsymbol{k}_1 + 2\cdot\boldsymbol{k}_2 + 2\cdot\boldsymbol{k}_3 + \boldsymbol{k}_4) + O(\Delta s^5). \tag{7}$$

After many steps, eqs. (6) and (7) provide a functional dependence between the initial and the final coordinates. Obviously it is almost impossible to write the dependence analytically, let alone differentiate the result in order to obtain the expansion of the transfer function. However, blindly performing all the operations in the steps of the Runge–Kutta algorithm in DA instead of real arithmetic, one automatically obtains the transfer function including all derivatives

$$\left(\partial^{(i+j+k+l+m+n)} r_p/\partial r_1^i\,\partial r_2^j\,\partial r_3^k\,\partial r_4^l\,\partial r_5^m\,\partial r_6^n\right)$$

with respect to the initial phase-space coordinates of eq. (3), i.e. the matrix elements $(r_p \mid r_1^i r_2^j r_3^k r_4^l r_5^m r_6^n)$. To this end, one simply must replace all quantities that depend

on the particle coordinates (with respect to which we want to differentiate) by DA vectors. In our case, this includes for instance the components of $\boldsymbol{r}$, and the three components of the flux density $\boldsymbol{B}$ in eq. (4), as well as the components of $\boldsymbol{F}$, $\boldsymbol{r}$ and $\boldsymbol{k}_i$ in eqs. (6) and (7). On the other hand, the quantities δ_K in eqs. (3), $\bar{p}/p_0$, $\bar{v}/v_0$ in eqs. (4) and η in eq. (5) as well as s and Δs in eq. (6) stay scalars.

4. Transfer matrices for the fringing fields of magnetic multipoles

To determine a transfer matrix for the fringing fields of magnetic multipole elements by solving the equations of motion using DA, it is necessary to first have an analytic description of the distribution of the flux density $\boldsymbol{B}$. Furthermore it is advantageous to replace this transfer matrix by one which describes field-free and main-field regions ranging up to the effective field boundary as well as a transfer across the effective field boundary [15,16].

4.1. The distribution of the flux density in multipole elements

In case of multipole elements [9,10,18] that have straight optic axes, it is advantageous to describe the distribution of the flux density $\boldsymbol{B}$ in cylindrical coordinates z, r and ϕ. Due to the time-independence and the fact that there are no currents inside the multipole element we infer from Maxwell's equations div $\boldsymbol{B}$ = curl $\boldsymbol{B} = 0$. Hence there exists a magnetic scalar potential V_B for which Laplace's equation holds, i.e. $\Delta V_B = 0$. This V_B can be expanded in a power series around $r = 0$ as

$$V_B(r, \phi, z) = \sum_{k=0}^{\infty} \sum_{l=0}^{\infty} M_{k,l}(z) \cos(l\phi + \theta_{k,l}) \cdot r^k. \tag{8}$$

Note that there is no power series expansion along the z-axis, i.e. the optic axis. In these cylindrical coordinates, Laplace's equation reads

$$\Delta V_B = \frac{1}{r} \frac{\partial}{\partial r}\left(\frac{r \cdot \partial V_B}{\partial r}\right) + \frac{1}{r^2} \frac{\partial^2 V_B}{\partial \phi^2} + \frac{\partial^2 V_B}{\partial z^2} = 0. \tag{9}$$

Inserting eq. (9) into eq. (8) one obtains

$$\Delta V_B = \sum_{k=0}^{\infty} \sum_{l=0}^{\infty} \left(M_{k,l}(k^2 - l^2) + M''_{k-2,l}\right) \times \cos(l\phi + \theta_{k,l}) \cdot r^{(k-2)} = 0, \tag{10}$$

where the double prime denotes the second derivative with respect to z.

In the main field of the multipole V_B is z-independent, causing $M''_{k-2,l}$ to vanish and eq. (10) to be fulfilled only for $l = k$. In this case eq. (8) simplifies to:

$$V_B(r, \phi) = \sum_{k=1}^{\infty} M_{k,k} \cos(k\phi + \theta_{k,k}) \cdot r^k.$$

For a multipole of $2k$-fold angular symmetry V_B thus increases with r^k, and the constant $M_{k,k}$ is the so-called multipole strength.

In the region of the fringing fields V_B depends on z. Thus the $M''_{k-2,l}$ do not vanish anymore and we can infer from eq. (10):

$$M_{k,l} = M''_{k-2,l}/(l^2 - k^2) \tag{11}$$

for $l \neq k$. Eq. (11) determines all $M_{k,l}$ from the z-derivatives of those with $l = k$. For an arbitrary superposition of multipoles we thus obtain from eqs. (8) and (11) to seventh order:

$$\begin{aligned} V_B(r, \phi) = {} & \sum_{k=2}^{\infty} \sum_{i=1}^{\infty} M_{k,k}^{(2i)}(z) \cdot r^{k+2i} \cdot \frac{k!}{i!(k+i)!(-4)^i} \\ & \cdot \cos(k\phi + \theta_{k,k}) \\ = {} & \left(M_{2,2} r^2 - M''_{2,2} \frac{r^4}{12} + M''''_{2,2} \frac{r^6}{384} + \cdots\right) \\ & \cdot \cos(2\phi + \theta_{2,2}) \\ & + \left(M_{3,3} r^3 - M''_{3,3} \frac{r^5}{16} + M''''_{3,3} \frac{r^7}{640} + \cdots\right) \\ & \cdot \cos(3\phi + \theta_{3,3}) \\ & + \left(M_{4,4} r^4 - M''_{4,4} \frac{r^6}{20} + \cdots\right) \\ & \cdot \cos(4\phi + \theta_{4,4}) \\ & + \left(M_{5,5} r^5 - M''_{5,5} \frac{r^7}{24} + \cdots\right) \\ & \cdot \cos(5\phi + \theta_{5,5}) \\ & + \left(M_{6,6} r^6 + \cdots\right) \cdot \cos(6\phi + \theta_{6,6}) + \cdots. \end{aligned} \tag{12}$$

Obviously eqs. (11) and (12) allow higher than kth-order r dependences to a $2k$-fold rotational symmetry. In the case of a pure quadrupole, i.e. for only $M_{2,2}$, $M''_{2,2}$, $M''''_{2,2}$, $\cdots$ being nonzero, there are thus contributions to the potential that obey the fourfold symmetry of the quadrupole but depend on r^2 as well as on r^4, r^6, $\cdots$. Note here that with larger and larger i the coefficients $k!/[i!(k+i)!4^i]$ decrease drastically while the magnitude of the derivatives of the multipole strengths $M_{k,k}^{(2i)}$ increase considerably, but that because of the increasing exponent of r the contribution to the potential V_B always decreases with increasing k for sufficiently small r.

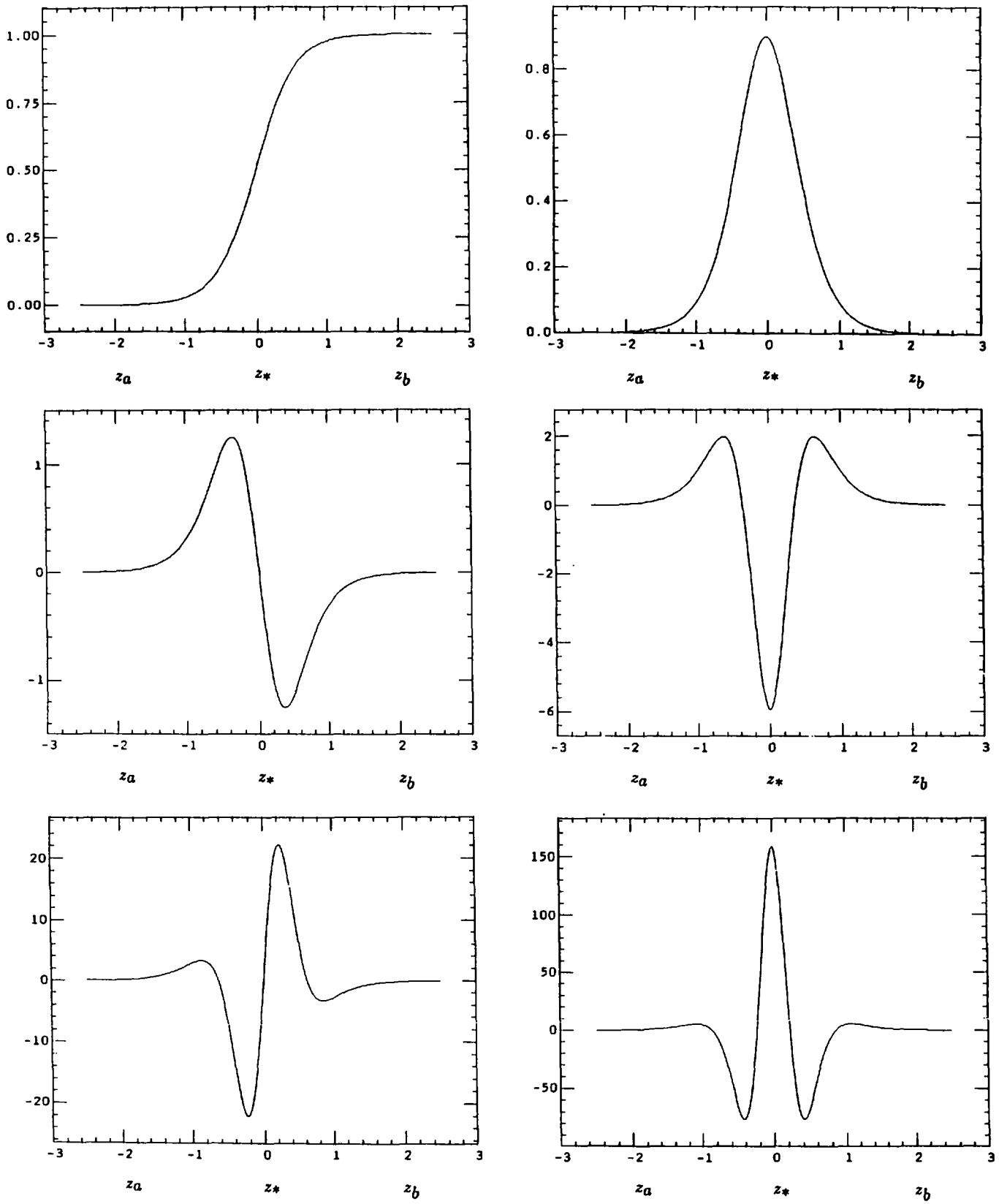

Fig. 1. The value and first five derivatives of the quadrupole strength as functions of the position on the optic axis. Note that at $z = z_a$ the value of $M_{2,2}$ is zero and has reached saturation at $z = z_b$. The curves shown were obtained by evaluating the function at different z values with fifth order DA. These results are required for eqs. (11) and (17).

4.2. The computation of fringing fields of magnetic multipoles

Since the distribution of the magnetic scalar potential, and thus of the flux density in magnetic multipoles, is uniquely determined by the values and the z-derivatives of the multipole strengths $M_{k,k}(z)$ (see eqs. (8) and (11)), it suffices to describe these multipole strengths as functions of z. All these multipole strengths vanish far outside the multipole, i.e. $M_{k,k}(z_a)=0$ in fig. 1, then increase in the fringing-field region, and finally reach a plateau of height $M_{k,k}(z_b)\neq 0$. This z-dependence of the strengths $M_{k,k}(z)$ of a multipole of aperture radius G_0 and of a main multipole strengths $M_{k,k}(z_b)$ can be described [33,21] by:

$$M_{k,k}(z) = \frac{M_{k,k}(z_b)}{1+\exp\left[b_{k,0}+b_{k,1}(z/G_0)+b_{k,2}(z/G_0)^2+\cdots\right]}, \tag{13}$$

which requires to fit the parameters $b_{k,j}$ to describe a given fringing-field distribution. Here z is assumed to be zero at the effective field boundary, so that the multipole strength at the effective field boundary is

$$M_{k,k}(z^*) = M_{k,k}(z_b)/[1+\exp(b_{k,0})].$$

The derivatives of multipole strengths, described by eq. (13), could be obtained analytically, even though for higher derivatives this procedure becomes quite cumbersome. Using DA, the derivatives are computed automatically by just evaluating the $M_{k,k}(z)$ in DA instead of in real numbers.

In the case of a permanent-magnet quadrupole the multipole strength $M_{2,2}(z)$ and consequently all its derivatives can be calculated analytically [14]. In this case the coefficients $b_{k,j}$ in eq. (13) are determined as $b_{2,0}=b_{2,2}=b_{2,4}=0.00000$ as well as:

$$b_{2,1}=3.59463, \qquad b_{2,3}=-0.09349, \qquad b_{2,5}=0.00106. \tag{14}$$

This quadrupole strength $M_{2,2}(z)$ and its derivatives to fifth order as obtained by DA are shown in fig. 1. Note that also the highest derivatives are accurate to machine precision. Using the thus obtained values of $M_{2,2}$, $M''_{2,2}$, $M''''_{2,2}$, etc. at a certain position z, the potential distribution in space can be determined from eq. (8). Consequently also the right hand side of eq. (2) can be determined and a solution of this differential equation be obtained using a Runge–Kutta method as in eqs. (6) and (7) from z_a to z_b in fig. 1.

In this connection one should mention that in order to obtain a description like eq. (13) for a real fringing field distribution, one should not only measure the $M_{k,k}(z)$ and fit the $b_{k,i}$ to those measurements, but one should also make the derivatives of eq. (13) match the derivatives of the $M_{k,k}(z)$.

One way to obtain these derivatives, which cannot easily be determined by measurements on the axis of the multipole element, is to measure the field on a closed surface, for instance the surface of a cylinder extending from the field-free to the main field region. As one sees from eq. (12), this potential – and analogously this field – contains information about the derivatives of the $M_{k,k}(z)$. However, this information cannot be recovered by Fourier transformation – which is often done in the case of the main fields – because several terms occur with the same angular dependence.

To avoid this problem, one here advantageously determines "surface charges" or "surface currents" on that surface such that they reproduce the measured scalar potential or field on that surface. The field given by the sum of the fields of all these surface charges and currents is fully Maxwellian and can be differentiated infinitely many times. Thus it can be used to determine the derivatives of the $M_{k,k}(z)$. By using this procedure, one computes derivatives that produce the proper field on the surface of the cylinder and hence have the right global behaviour.

In the majority of cases, however, it is sufficient to determine the $b_{k,i}$ as accurately as is easily possible by just fitting eq. (13) to the measured $M_{k,k}(z)$. The flux density distribution obtained in this fashion fulfills Maxwell's equations everywhere, though it is not the one that one really looks out for, but one that would be produced from slightly different pole faces. However, typically the difference between this distribution and the one one would obtain in some accurate measurement of the flux density caused by the real pole faces is smaller than the commonly achievable fabrication accuracy.

Furthermore, it should be noted that since the function in eq. (13) is rather smooth, it is likely that it will produce too small derivatives and hence too smooth fields on average. However, even if this happens, the erroneous higher derivatives due to the fitting do not influence the transfer map very much. A local error in the $M_{k,k}(z)$ produces localized higher derivatives which tend to oscillate around the true solution while in the integration process to determine the transfer map such localized oscillations usually average out to a large extent and do not affect the aberrations drastically.

4.3. Fringing-field transfer matrices across an effective field boundary

Though in principle the motion of charged particles in the fringing field is fully described as soon as one has obtained the transfer matrix from z_a to z_b in fig. 1, it is advantageous [16] to replace the transfer matrix from z_a to z_b by the product of three transfer matrices:

1) a transfer matrix for a field-free region, ranging from z_a to z^*, i.e. to the position of the effective field boundary;
2) a transfer matrix which is located at the effective field boundary and which summarizes all fringing-field effects;
3) a transfer matrix for a region ranging from z^* to z_b, in which the multipole strength is assumed to be constant.

In this case the elements of the center transfer matrix must be chosen such that the product of all three transfer matrices is equal to the fringing-field transfer matrix from z_a to z_b. This center transfer matrix is usually called [16,26] "the fringing-field transfer matrix".

The reason for describing the fringing-field action by this "fringing-field transfer matrix" [15,16] is that, as long as Laplace's equation is assumed to be valid throughout the fringing field, in this matrix

1) several of the elements – though being large – become independent of the specific fringing-field distribution,
2) many elements vanish altogether,
3) many elements that depend on the detailed distribution of the fringing field are small.

Thus in this case a rough description of the distribution of the fringing-field is adequate even for a quite precise description of the fringing-field action.

The small matrix elements that depend on the detailed distribution of the fringing field can all be expressed by integrals over the extent of the fringing field, i.e. over Δz. Assuming that z is of the same magnitude as the diameter of the particle beam, only those integrals must be taken into account into which Δz enters to the $1, 2, \cdots, n-1$ power, if the transfer matrix shall be of the nth order. In case of a magnetic quadrupole, i.e. $k = 2$, these integrals are [18]:

$$I_1 \cdot G_0^2 = \int_{z_a}^{z_b} \int_{z_a}^{z} \frac{M_{2,2}(\bar{z})}{M_{2,2}(z_b)} \, d\bar{z} \, dz - \frac{z_b^2}{2} = 0.13852,$$

$$I_2 \cdot G_0^3 = \int_{z_a}^{z_b} z \left[\int_{z_a}^{z} \frac{M_{2,2}(\bar{z})}{M_{2,2}(z_b)} \, dz \right] dz - \frac{z_b^3}{3} = 0.00000,$$

$$I_3 \cdot G_0^3 = \int_{z_a}^{z_b} \left[\int_{z_a}^{z} \frac{M_{2,2}(\bar{z})}{M_{2,2}(z_b)} \, d\bar{z} \right]^2 dz - \frac{z_b^3}{3} = 0.0660,$$

$$I_4 \cdot G_0 = \int_{z_a}^{z_b} \left[\frac{M_{2,2}(z)}{M_{2,2}(z_b)} \right]^2 dz - z_b = -0.28501.$$

Here z_a is a point outside of the quadrupole field and z_b denotes a point in the main region of the quadrupole. The numerical numbers given above correspond to the fringing field of a permanent magnet quadrupole as described by the $b_{2,k}$ of eq. (14). Furthermore $M_{2,2}(z_b)$ is the quadrupole strength in the main region of the quadrupole of aperture radius G_0 and $M_{2,2}(z)/M_{2,2}(z_b)$ is the relative quadrupole strength in the fringing field.

4.4. Comparison between third-order fringing-field transfer matrices

In all our simulations the reference particle was chosen to be singly charged having a mass of 200 mass units and an energy of 100 keV. For such particles we used DA to compute the fifth-order transfer map of the main field of quadrupoles, hexapoles, octupoles, decapoles and duodecapoles. These results can be compared with the analytical formulas in the libraries of COSY [22,23] yielding agreement of at least seven significant digits for all matrix elements of magnetic multipoles of up to fifth order [13]. By using a smaller step size in the Runge-Kutta integrator, the number of digits in agreement could probably be increased further. This result is similar to the comparison [28] between DA and the code TEAPOT.

In the case of the matrix elements for the fringing-field region we tested the transfer matrix of a magnetic quadrupole, the relative quadrupole strength $M_{2,2}(z)/M_{2,2}(z_b)$ of which we chose to be given by eqs. (13) and (14). In detail we chose different values of the aperture radius G_0 as well as of the quadrupole strength $M_{2,2}(z_b)$ in the main region. The left column of plots in fig. 2 shows the dependence of the first-order matrix elements and of some selected high-order matrix elements on the quadrupole strength $M_{2,2}(z_b)$ which is varied between 0 and 1 T/m assuming a fixed aperture radius of $G_0 = 0.05$ m. The right column of plots in fig. 2 shows the dependence of the same matrix elements on the aperture radius G_0 which is varied between 1 and 12 cm assuming a fixed quadrupole strength $M_{2,2}(z_b) = 0.5$ T/m.

All matrix elements of first and second order obtained by using the fringing-field integral method approximate the DA values of the matrix elements quite well. In the cases shown here, the differences between the results obtained by both methods and the sharp cut-off approximation are at most about 10% and typically $< 1\%$ or they are very small to begin with. Note, however, that the sharp cut-off approximation, as used in most ion-optics codes, produces considerable deviations from the more accurate two other results. For the matrix elements of third-order the sharp cut-off approximation yields the same results as the fringing-field integral method which assumes that the extent of the fringing field is taken into account to the same power as the highest terms in the transfer matrix.

5. Transfer matrices for the fringing fields of sector magnets

Also in the case of sector magnets a detailed description of the distribution of the flux density $\boldsymbol{B}$ is a

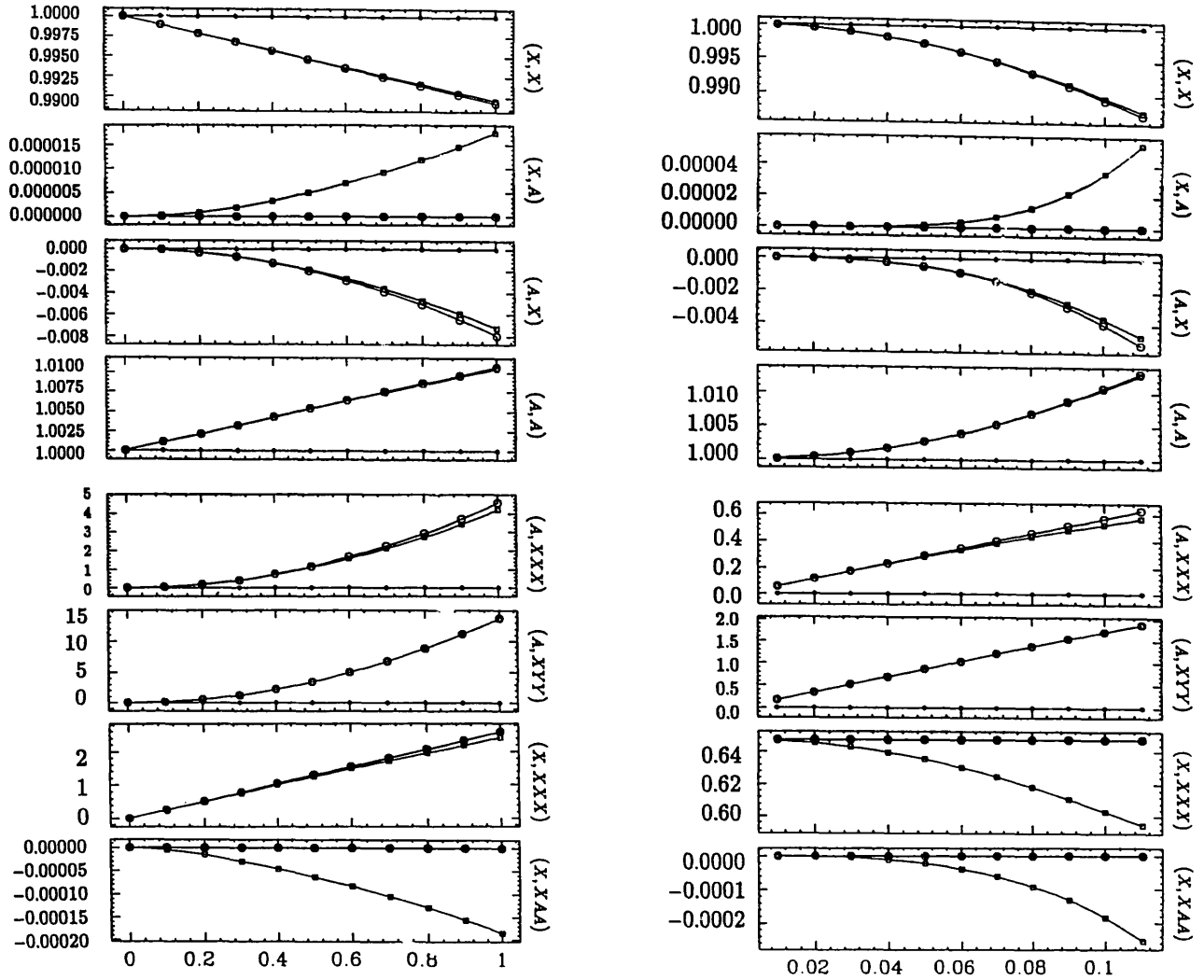

Fig. 2. The magnitude of the elements (X, X), (X, A), (A, X) and (A, A) as well as the elements (A, XXX), (A, YYY), (X, XXX), (X, XAA) of a quadrupole fringing-field transfer matrix, i.e. a transfer matrix that transfers a particle trajectory across the effective-field boundary are shown. These elements were calculated assuming singly charged particles of 200 mass units and 100 keV energy. Shown are the "exact results" obtained by DA (circles), the results obtained by the fringing-field integral method (squares) and the results obtained from the sharp cut-off approximation (diamonds). For the left column of the drawings the aperture radius was chosen to be $G_0 = 0.05$ m and the quadrupole strength $M_{2,2}(z_b)$ has been varied between 0 and 1 T/m. The right column of drawings shows the same matrix elements assuming a fixed quadrupole strength $M_{2,2}(z_b) = 0.5$ T/m and aperture radii G_0 varied between 0.01 and 0.11 m. Note here that using the fringing-field integral method the first-order matrix elements are:

$$(X, X) = 1 - K^2 I_1, \quad (X, A) = -2K^2 I_2, \quad (A, X) = -K^4 I_3, \quad (A, A) = 1 + K^2 I_1$$

with $K^2 = (q/p) M_{2,2}(z_b)$ according to ref. [18], and in the sharp cut-off approximation these elements are the same, however, with $I_1 = I_2 = I_3 = I_4 = 0$.

prerequisite for obtaining matrix elements by using DA. While the procedure has a similar flavor as in section 4, here things are a little more complicated.

For all sector magnets, the ion-optical properties of which we want to describe, we assume the optical axis to be a circle of radius ρ_0 inside the main field, and the coordinate along this axis is denoted as z. In the region of the main field this entails that the flux density $\boldsymbol{B}$ along this circle is $B_0 = \text{constant}$, i.e. independent of z, and thus the pole faces are rotationally symmetric. In the plane of the optic axis, i.e. for $y = 0$, then the y-component of the flux density distribution is described by [4,5]:

$$\frac{B_y(x)}{B_0} = 1 - \sum_{i=1}^{\infty} \left(\frac{n_i x^i}{i!} \right),$$

with x describing the deviation of a trajectory from the optic axis and the n_i being coefficients that describe the inhomogeneity of the field distribution. This description of $B_y(x)$ includes that of a homogeneous magnet, having parallel pole faces and a flux density distribution $B_y(x) = B_0$, i.e. all n_i vanish.

In the fringing field such relations are more complicated. As in the case of multipoles we infer from Maxwell's equations div $\boldsymbol{B} = \text{curl } \boldsymbol{B} = 0$ due to the time-independence and the fact that there are no currents inside the sector magnet. Hence also here exists a magnetic scalar potential V_B for which Laplace's equation holds, i.e. $\Delta V_B = 0$. We may also expand this potential in particle-optical coordinates x and y keeping the z-dependence unexpanded. In detail one can write:

$$V_B(x, y, z) = \sum_{i=0}^{\infty} \sum_{j=0}^{\infty} a_{i,j}(z) \frac{x^i}{i!} \frac{y^j}{j!} \tag{15}$$

and postulate because $\Delta V_B = 0$ [34,6]:

$$\nabla^2 V_B = \frac{1}{1+hx} \frac{\partial}{\partial x}\left((1+hx)\frac{\partial V_B}{\partial x}\right) + \frac{\partial^2 V_B}{\partial y^2} + \frac{1}{1+hx} \frac{\partial}{\partial z}\left(\frac{1}{1+hx}\frac{\partial V_B}{\partial z}\right) = 0. \tag{16}$$

Here $h(z) = 1/\rho$ is the momentary radius of curvature of the optic axis. Since sector magnets all have midplane symmetry, $V_B(x, y, z)$ must equal $V_B(x, -y, z)$ and all coefficients $a_{i,j}$ with even j must vanish. Note also that for a homogeneous magnet all $a_{i,j}$ vanish except $a_{0,1}$. Inserting eq. (15) into eq. (16) one obtains furthermore:

$$\begin{aligned} a_{i,j+2} = &- a''_{i,j} - iha''_{i-1,j} + ih'a'_{i-1,j} - a_{i+2,j} \\ &- (3i+1)ha_{i+1,j} - 3iha_{i-1,j+2} \\ &- i(3i-1)h^2 a_{i,j} - 3i(i-1)h^2 a_{i-2,j+2} \\ &- i(i-1)^2 h^3 a_{i-1,j} \\ &- i(i-1)(i-2)h^3 a_{i-3,j+2}, \end{aligned} \tag{17}$$

where primes denote derivatives with respect to z, and it is understood that all coefficients with negative indices are zero. In the main field region of the sector magnet the potential V_B is independent of z, causing all z derivatives to vanish so that eq. (17) simplifies considerably to

$$a_{i,j+2} = -a_{i+2,j} - ia_{i-1,j} - (i+1)a_{i+1,j}. \tag{18}$$

Since all $a_{i,j}$ vanish for even j eqs. (17) and (18) allow to determine all $a_{i,j}$ once all $a_{i,1}$ are known. Thus Laplace's equation determines the potential V_B up to a constant in all space, once its first y-derivative at $y = 0$ is known in a power series in x for all z. Consequently one finds to second order with $h = h(z)$.

$$\begin{aligned} B_x(x, y, z) &= -\left(\frac{\partial V_B(z)}{\partial x}\right) \\ &= -a_{11}(z)y - a_{21}(z)xy + \cdots, \\ B_y(x, y, z) &= -\left(\frac{\partial V_B}{\partial y}\right) \\ &= -a_{01}(z) - a_{11}(z)(x - \tfrac{1}{2}hy^2) \\ &\quad - \tfrac{1}{2}a_{21}(z)(x^2 - y^2) + \tfrac{1}{2}a_{01}(z)''y^2 \\ &\quad + \cdots, \\ B_z(x, y, z) &= \frac{-1}{1+hx}\left(\frac{\partial V_B}{\partial z}\right) \\ &= \frac{-1}{1+hx}(a'_{01}(z)y + a'_{11}(z)xy + \cdots). \end{aligned}$$

5.1. The computation of fringing fields of sector magnets

In case of the fringing fields of sector magnets, the momentary curvature of a particle trajectory under investigation as projected onto the plane of the optic axis ($y = 0$) depends on the position s along the particle trajectory. This curvature varies as $B_y(s)$, both being zero far outside the magnet and then increasing monotonically to reach a plateau inside the magnet.

In a Cartesian coordinate system X, Y, Z the distributions of the scalar magnetic potential $V_B(X, Y, Z)$ and thus of the flux density $\boldsymbol{B}(X, Y, Z)$ are uniquely determined by the distribution of $B_Y(X, 0, Z)$ i.e. the Y-component of the flux density in the magnet midplane at $Y = 0$. In order to find $B_Y(X, Y, Z)$ at an arbitrary point $P(X, Y, Z)$ it thus is only necessary to determine $B_Y(Z, 0, Z)$ at $P(X, 0, Z) = P(X, Z)$ in the plane of the optic axis $Y = 0$. In detail we follow a procedure outlined in ref. [33]:

1) Look for the closest point $P_0(X, Z)$ on the effective field boundary (see fig. 3) and determine the distance d between P and P_0.

2) Determine the distance ρ between $P_0(X, Z)$ and M, the center of the circular optic axis, and find the flux density for a point inside the sector magnet with the same distance ρ from M:

$$B_Y(\rho) = a_{0,1} + a_{1,1}\frac{\rho - \rho_0}{1!} + a_{2,1}\frac{(\rho - \rho_0)^2}{2!} + \cdots,$$

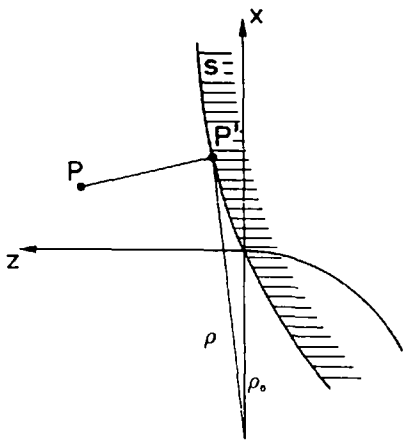

Fig. 3. Illustration for the computation of the midplane fringe field in a sector magnet according to the "Enge procedure" [33]. For details, refer to the text.

where ρ_0 is the radius of the optic axis. Note here that in the case of a homogeneous magnet $B_Y = a_{0,1}$ independently of ρ.

3) Determine the flux density at point P_0 from

$$B_Y(X, 0, Z) = \frac{B_Y(\rho)}{1 + \exp\left[b_0 + b_1(d/G_0) + b_2(d/G_0)^2 + \cdots\right]}, \tag{19}$$

where in advance the b_i must be fitted to the given flux density distribution in the fringing field. Here Z is assumed to be zero at the position where the optic axis crosses the effective field boundary so that the flux density at this point is $B_Y(X, 0, 0) = B_Y(\rho)/[1 + \exp(b_0)]$.

In case the effective field boundary is curved by a radius R, it is in general impossible to find a closed expression for the distance d; instead, d must be determined iteratively. To do this, one notes that it is a necessary condition that the line (PP_0) is perpendicular to the tangent of the effective field boundary S at $P_0(X_0, Z_0)$, which is given by $[1, S'(X_0)]$, i.e.:

$$[X - X_0, Z - S(X_0)] \cdot [1, S'(X_0)] = 0. \tag{20}$$

Writing the function $S(X_0)$ as a polynomial $S(X_0) = S_1 X_0 + S_2 X_0^2 + \cdots$ and inserting this polynomial into eq. (20), one obtains the iterative form

$$X_0 = \{X + Z(S'(X_0) - 2S_2 X_0) - (S(X_0)S'(X_0) - S_1^2 X_0)\} \times \{1 + S_1^2 - 2ZS_2\}^{-1}.$$

A closer inspection of the right hand side shows that there are no linear terms in x left, which entails quadratic convergence. Iterating this equation one finally obtains the position $P_0(X_0, Z_0)$, and from that the distance d.

In order to obtain the required derivatives of the midplane field parallel and perpendicular to the optic axis, we also used DA. To be more specific, the coordinates X_0 and Z_0 of P_0 are not interpreted as real numbers anymore, but are viewed as DA quantities depending on x and y. Replacing all the operations to determine X and Y by the corresponding ones in DA, including the iteration process to determine the point P_0 one automatically obtains the derivatives of the field with respect to x and y, i.e., the derivatives along the optic axis and in the midplane perpendicular to the optic axis. So we obtain the terms $a_{i,1}$ and all their derivatives with respect to s. This then enables us to compute the flux density $\boldsymbol{B}$ along the particle trajectory under consideration by using the recursive formula of eq. (17).

5.2. Fringing-field transfer matrices across an effective field boundary

The distribution of the flux density $b_y(s)$ along a particle trajectory in the fringing field of a sector magnet looks very similar to the distribution of the quadrupole strength shown in fig. 1. Also here we will first determine a transfer matrix and transfers a particle trajectory from s_a to s_b – corresponding to z_a and z_b in fig. 1 – and then extract from this a transfer matrix that summarizes all left-over effects at the effective field boundary, the so-called "fringing-field transfer matrix" which has similar properties as listed in section 4.3.

Also here the small matrix elements that depend on the detailed distribution of the fringing field can be expressed by integrals over the extent of the fringing field. Assuming that $\Delta s = s_b - s_a$, i.e. the extent of the fringing field, is of the same magnitude as the diameter of the particle beam, only those integrals must be taken into account into which Δs enters to $1, 2, \cdots, n-1$ order, if the transfer matrix shall be of nth order. In case of a sector magnet these integrals are [15–17]:

$$I_1 \cdot G_0^2 = \int_{\zeta_a}^{\zeta_b}\int_{\zeta_a}^{\zeta} \frac{B_y(\bar{\zeta})}{B_0} \mathrm{d}\bar{\zeta}\, \mathrm{d}\zeta - \frac{\zeta_b^2}{2} = 0.13852,$$

$$I_2 \cdot G_0 = \int_{\zeta_a}^{\zeta_b} \left[\frac{B(\zeta)}{B_0}\right]^2 \mathrm{d}\zeta - \zeta_b = -0.28501,$$

$$I_3 \cdot G_0^3 = \int_{\zeta_a}^{\zeta_b} \zeta \frac{B(\zeta)}{B_0} \mathrm{d}\zeta = -0.06930.$$

Here ζ is a coordinate perpendicular to the effective field boundary at the position where he optic axis is assumed to cross the effective field boundary. Analogously to the fringing field integrals of section 4.3 here ζ_a denotes a point outside the dipole field and ζ_b a point in the main field region. For convenience the numerical values listed for the above three fringing-field integrals are obtained from choosing the numerical values of the b_i in eq. (19) to be identical to the $b_{k,l}$ of eqs. (13) and (14) though such a fringing-field distribution is not easily found in a sector magnet.

5.3. Comparison between third-order fringing-field transfer matrices

For a numerical analysis we assumed that in the sector magnet under consideration the optic axis would be a circle of 2.5 m radius. Also here we used DA to compute the fifth-order transfer map fo the main field and compared the results with the analytical formulas in the libraries of COSY [22,23] again finding agreement of at least seven significant digits for all matrix elements of sector magnets up to fifth order. Also here we assume that by using a smaller step size in the Runge–Kutta integrator, the number of digits in agreement could probably be increased further.

In the case of the matrix elements of the fringing-field transfer matrix for a sector magnet we varied G_0, the half gap of the magnet, as well as the entrance angle ϵ, i.e. the angle between the optic axis and the effective field boundary. The left column of plots in fig. 4 shows the dependence of two first-order matrix elements and of seven selected high-order matrix elements on G_0 with this half gap size being varied from 0.01 to 0.11 m while the entrance angle was kept fix at $\epsilon = 0°$. The right column of plots in fig. 4 shows for a fixed $G_0 = 0.05$ m the dependence of the same matrix elements on the entrance angle ϵ, with ϵ being varied between $+60°$

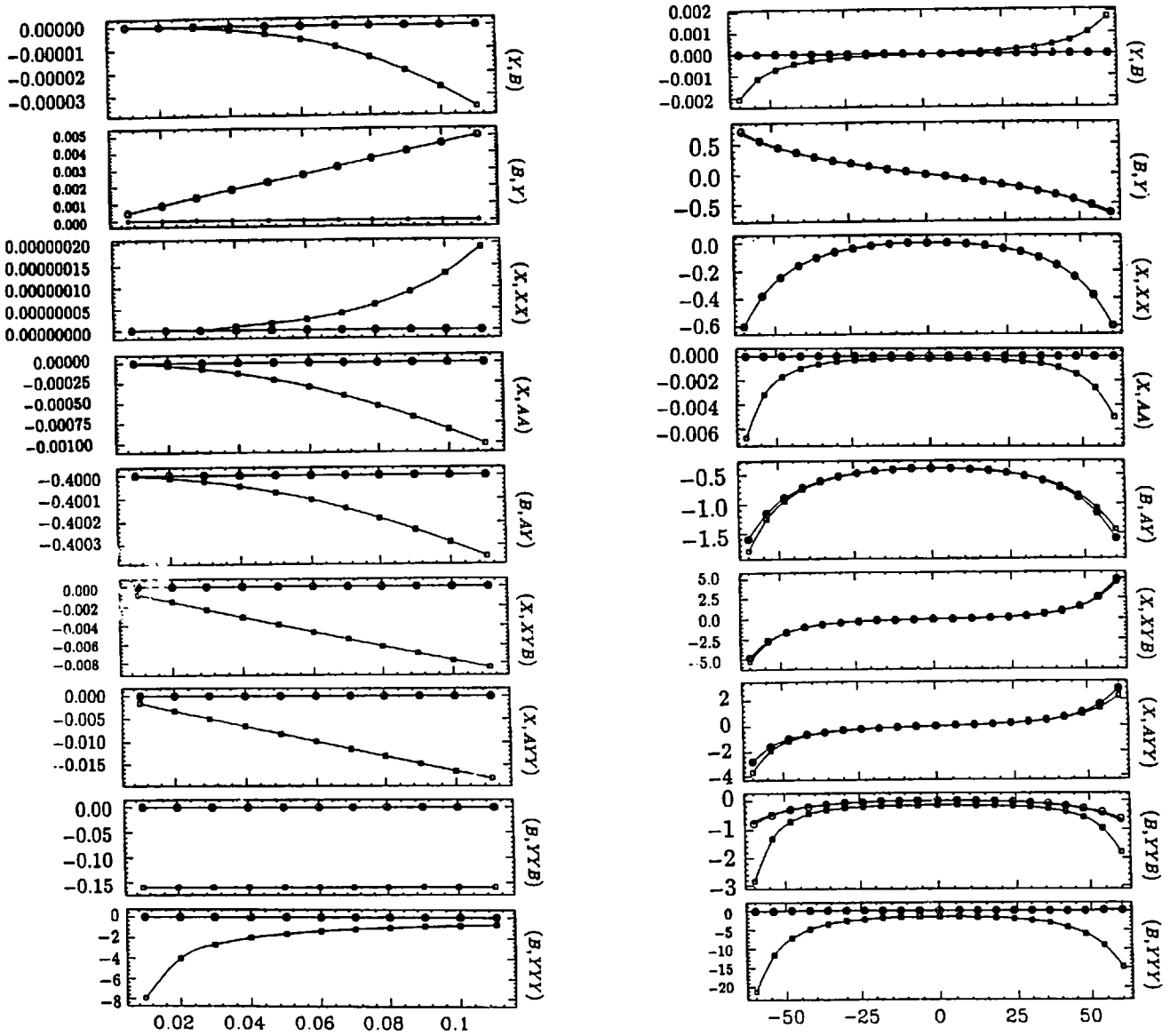

Fig. 4. The magnitude of the elements (Y, B) and (B, Y) as well as (X, XX), (X, AA), (B, AY), (X, XYB), (X, AYY), (B, YYB), (B, YYY) are shown of a sector magnet fringing-field transfer matrix, i.e. a transfer matrix that transfers a particle trajectory across the effective-field boundary. These elements were calculated assuming a homogeneous magnet with an optic axis of 2.5 m radius. Shown are the "exact results" obtained by differential algebra (circles), the results obtained by the fringing-field integral method (squares) and the results obtained from the sharp cut-off approximation (diamonds). For the left hand column of drawings the entrance angle ϵ was chosen to be 0° and the half gap of the magnet varied from $G_0 = 0.01$ to $G_0 = 0.11$ m. For the right hand column the half gap of the magnet was chosen to be $G_0 = 0.05$ m and the angle of inclination varied between $\epsilon = \pm 60°$. Note here that the first-order matrix elements determined with the fringing-field integral method are:

$$(X, X) = (Y, Y) = 1, \qquad (X, A) = -2\rho_0 I_1 \tan(\epsilon)/\cos^2(\epsilon),$$

$$(A, X) = -(B, Y) = \rho^{-1} \tan(\epsilon) \qquad (A, A) = 1 - 2I_1 \tan(\epsilon)/\cos^2(\epsilon)$$

according to refs. [18,18] and that in the sharp cut-off approximation these elements are the same, however, with $I_1 = I_2 = I_3 = 0$.

and $-60°$ though for simply designed magnets this angle should only be varied between $+30°$ and $-30°$.

All matrix elements of first and second order, obtained by using the fringing-field integral method, approximate the DA values of the matrix elements quite well. For the matrix elements of third-order the sharp cut-off approximation here also yields the same results as the fringing-field integral method since this assumes Δs, the extent of the fringing field, to be of equal magnitude as the diameter of the particle beam. Note, however, that the scales on the drawings of the left hand column are considerably smaller than those on the drawings of the right hand column. This reflects the fact that the influence of the fringing fields on the matrix elements is small as long as the particle beam enters into the sector magnet more or less perpendicular, but that this influence becomes large if the particle beam enters obliquely. Note also that there are matrix elements like (B, YYY) that grow drastically if G_0, the half gap of the magnet, becomes very small compared to the radius of the optic axis as for instance in a large ring accelerator or storage ring.

Acknowledgements

We are indebted to Dr. H. Nestle and H.-C. Hofmann for fruitful discussions about questions of symmetry in multipole fields and to S. Meuser for help in testing subroutines of the used DA package.

References

[1] K.L. Brown, R. Belbeoch and P. Bounin, Rev. Sci. Instr. 35 (1964) 481.
[2] H. Wollnik, Nucl. Instr. and Meth. 52 (1967) 250.
[3] H. Hintenberger and L.H. König, Z. für Naturfg. 12a (1957) 773.
[4] A.J.H. Boerboom, H.A. Tasman and A. Wachsmuth, Z. für Naturfg. 14a (1958) 121, 816, 818.
[5] H. Wollnik, Nucl. Instr. and Meth. 34 (1965) 213.
[6] K.L. Brown, Techn. Rep. 91, SLAC (1979).
[7] R. Ludwig, Z Naturfg. 22a (1967) 553.
[8] T. Matsuo and H. Matsuda, Int. J. Mass. Spectr. Ion Phys. 6 (1971) 361.
[9] D. Smith, Nucl. Instr. and Meth. 79 (1970) 144.
[10] E. Lee Whiting, Nucl. Instr. and Meth. 83 (1970) 232.
[11] A.J. Dragt, L.M. Healy, F. Neri and R. Ryne, IEEE Trans. Nucl. Sci. NS-35 (1985) 2311.
[12] M. Berz and H. Wollnik, Nucl. Instr. and Meth. A258 (1987) 364.
[13] M. Berz and H. Wollnik, AIP Conf. Proc. 177 (1988) 301.
[14] K. Halbach, Nucl. Instr. and Meth. 187 (1981) 109.
[15] H. Wollnik and H. Ewald, Nucl. Instr. and Meth. 36 (1965) 93.
[16] H. Wollnik, Nucl. Instr. and Meth. 38 (1965) 56.
[17] H. Matsuda and H. Wollnik, Nucl. Instr. and Meth. 77 (1970) 40.
[18] H. Matsuda and H. Wollnik, Nucl. Instr. and Meth. 103 (1972) 117.
[19] T. Matsuo, H. Matsuda, Y. Fujita and H. Wollnik, Mass. Spectr. 24 (1976).
[20] M. Berz, H. Wollnik, J. Brezina and W. Wendel, Proc. AMCO-7, GSI-Rep. THD-26 (1984) p. 679.
[21] H. Wollnik, J. Brezina and M. Berz, Nucl. Instr. and Meth. A258 (1987) 408.
[22] M. Berz, H.C. Hofmann and H. Wollnik, Nucl. Instr. and Meth. A258 (1987) 402.
[23] H. Wollnik, B. Hartmann and M. Berz, AIP Conf. Proc. 177 (1988) 74.
[24] A.J. Dragt, AIP Conf. Proc. 87 (1982).
[25] H. Wollnik and M. Berz, Nucl. Instr. and Meth. A238 (1985) 127.
[26] H. Wollnik, Charged Particle Optics (Academic Press, Orlando, FL, 1987).
[27] M. Berz, Nucl. Instr. and Meth. A258 (1987) 431.
[28] M. Berz, AIP Conf. Proc. 177 (1988) 275.
[29] M. Berz, Part. Accel. 2 (1989).
[30] D. Laugwitz, Jahresber. der Deutschen Math. Ver. 75 (1973) 66.
[31] M. Berz, AIP Conf. Proc. 1 (1989) 961.
[32] M. Berz, IEEE Trans. Electron Devices. ED. 35 (1988) 11.
[33] S. Kowalski and H. Enge, Tech. Rep., MIT, Cambridge, MA (1985).
[34] L.C. Teng, Tech. Rep. ANL-LCT-28, ANL (1962).